



## Editor's Choice

# Wave packet bifurcation in ultrafast hydrogen migration in $\text{CH}_3\text{OH}^+$ by pump-probe coincidence momentum imaging with few-cycle laser pulses



Toshiaki Ando<sup>a</sup>, Akihiro Shimamoto<sup>a</sup>, Shun Miura<sup>a</sup>, Katsunori Nakai<sup>a</sup>, Huailiang Xu<sup>b</sup>, Atsushi Iwasaki<sup>a</sup>, Kaoru Yamanouchi<sup>a,\*</sup>

<sup>a</sup> Department of Chemistry, School of Science, The University of Tokyo, 7-3-1 Hongo, Bunkyo-ku, Tokyo 113-0033, Japan

<sup>b</sup> State Key Laboratory on Integrated Optoelectronics, College of Electronic Science and Engineering, Jilin University, Changchun 130012, China

## ARTICLE INFO

## Article history:

Received 19 January 2015

In final form 9 February 2015

Available online 17 February 2015

## ABSTRACT

Ultrafast nuclear dynamics in  $\text{CH}_3\text{OH}^+$  has been studied based on the released kinetic energy distributions of the fragment ions in the non-migration ( $\text{CH}_3\text{OH}^{2+} \rightarrow \text{CH}_3^+ + \text{OH}^+$ ) and migration ( $\text{CH}_3\text{OH}^{2+} \rightarrow \text{CH}_2^+ + \text{OH}_2^+$ ) pathways obtained by pump-probe coincidence momentum imaging with few-cycle laser pulses ( $6.0(5)$  fs,  $2.1(2) \times 10^{14}$  W/cm<sup>2</sup>). A characteristic oscillatory structure with a bifurcation at  $\sim 150$  fs in the kinetic energy distribution of the migration pathway is interpreted as the motion of a vibrational wave packet on a bound well around the migrated geometry, oscillating first along the C–O bond and bifurcating into bound and dissociating components.

© 2015 Elsevier B.V. All rights reserved.

## 1. Introduction

Our recent studies [1–5] have revealed that ultrafast hydrogen migration processes are induced in hydrocarbon molecules when they are irradiated with ultrashort intense laser pulses. In all cases of  $\text{CH}_3\text{CN}$  [1],  $\text{CH}_3\text{OH}$  [2] and  $\text{C}_3\text{H}_4$  (allene) [3,4], hydrogen migration processes were induced efficiently by the irradiation of femtosecond laser pulses whose pulse durations were ranged between 40 and 70 fs. In these studies, however, it remained unclear whether the migration proceeded in the singly or higher charged parent species, because the hydrogen migration within a parent molecule and its multiple ionization were both induced within the duration of the laser pulses.

In 2010, we investigated the hydrogen migration in  $\text{CH}_3\text{OH}$  at real time by measurements of pump-probe coincidence momentum imaging (CMI) using femtosecond laser pulses whose duration was 38 fs, and we were able to find that the hydrogen migration proceeds in  $\text{CH}_3\text{OH}^+$ , and that there are two different time scales in the hydrogen migration: (i) faster hydrogen migration having completed already at the shortest pump-probe time delay at 100 fs and (ii) slower hydrogen migration with a time constant of  $\sim 150$  fs [5]. In order to investigate how fast the faster hydrogen migration

proceeds, it was necessary to use much shorter laser pulses in the pump-probe measurements.

In the present study, we have generated few-cycle laser pulses with pulse durations as short as 6 fs, and by using the few-cycle laser pulses, we have performed pump-probe CMI measurements of hydrogen migration processes in  $\text{CH}_3\text{OH}^+$ . We have thus detected the fragment ions produced by the following two Coulomb explosion pathways:

*Non-migration pathway*



*Migration pathway*



and recorded the distribution of the released kinetic energies as a function of the pump-probe time delay ranging between  $-20$  and  $500$  fs.

For the non-migration pathway, we find that the C–O bond breaking,



proceeds via the energized states in the first electronically excited  $\tilde{A}$  state. For the migration pathway, we have found that a nuclear wave packet flows from the higher electronic states than the  $\tilde{A}$  state in the non-migrated geometrical configuration into the bound well of the migrated geometrical configuration, and oscillates first along

\* Corresponding author.

E-mail address: [kaoru@chem.s.u-tokyo.ac.jp](mailto:kaoru@chem.s.u-tokyo.ac.jp) (K. Yamanouchi).

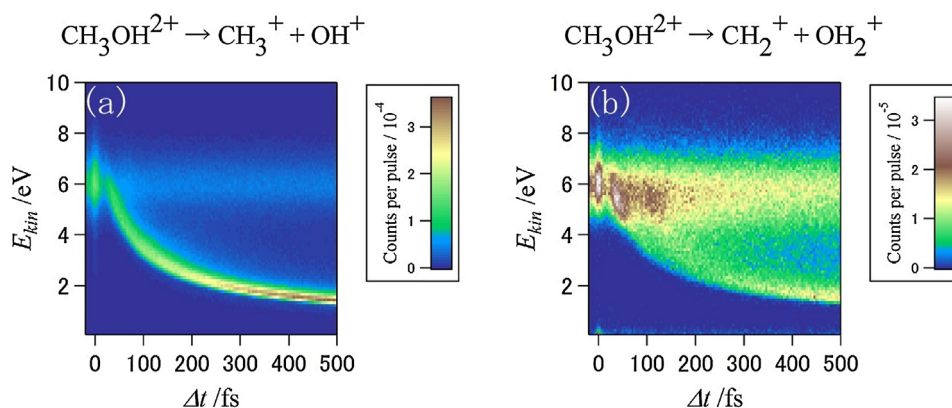


**Figure 1.** The  $E_{\text{kin}}$  distributions in the non-migration pathway (a) and the migration pathway (b) as a function of  $\Delta t$ . The number of the counts in each time bin whose width is 4 fs is normalized by the total number of the laser shots in the bin. The width of the time bin is set to be slightly shorter than the laser pulse duration ( $\sim 6$  fs).

the C–O bond, and then bifurcates at  $\sim 150$  fs into the bound component and the dissociative component that leads to the C–O bond breaking,



## 2. Experimental

The experimental setup for the generation of linearly polarized few-cycle laser pulses and the detection of fragment ions have been described previously [6]. The experimental setup consists of (i) a chirped-pulse-amplification femtosecond Ti:sapphire laser system, (ii) a pulse compression system to generate few-cycle laser pulses [7] and (iii) an ultrahigh vacuum chamber for CMI measurements [8]. Output pulses of the femtosecond laser system (800 nm, 5 kHz, 0.6 mJ, 30 fs) were focused into a hollow-core fiber (1.5 m long, 330  $\mu\text{m}$  inner diameter) filled with an Ar gas (0.4 atm) to induce the self-phase modulation. After passing through the fiber, the spectral bandwidth of the laser pulses became  $\sim 300$  nm at full-width at tenth-maximum at the center wavelength of 770 nm. The spectral phase dispersion was compensated by chirp mirrors (PC70, Ultrafast Innovations) and a pair of wedged fused silica plates for few-cycle laser pulses, which were characterized by a home-built two-dimensional spectral shearing interferometer [9]. The few-cycle laser pulses were then introduced into a Michelson interferometer to generate pump and probe laser pulses, and the optical time delay  $\Delta t$  of a probe laser pulse measured from a pump laser pulse was varied using a piezo-controlled optical stage. The pulse duration were measured to be 6.0(5) fs. The piezo stage is controlled by a function generator and  $\Delta t$  is scanned from  $-20$  fs to 500 fs at 0.01 Hz to cancel out the effect of long term fluctuations in the sample gas density as well as in the spatiotemporal profile of laser pulses. The pump and probe laser pulses were both focused by a concave mirror ( $f=150$  mm) placed in the vacuum chamber onto an effusive molecular beam of methanol ( $\text{CH}_3\text{OH}$ ) vapor, whose rotational temperature is estimated to be the same as room temperature. The polarization directions of pump and probe laser pulses were set to be parallel to the propagation axis of the molecular beam.

The fragment ions generated from  $\text{CH}_3\text{OH}$  were guided by a static electric field toward a two-dimensional position sensitive detector (HEX120, RoentDek) in the velocity map imaging configuration. The momentum vectors of the fragment ions were determined from the flight time and the positions of the fragment ions. For every laser shot, the momentum data of the fragment ions and the delay time data were collected simultaneously by a data acquisition board (TDC8HP, RoentDek). By imposing coincidence conditions on the momentum and delay time data, two-body Coulomb explosion pathways (1) and (2) were extracted, and the

released kinetic energies obtained from the momenta of fragment ion pairs were plotted as a function of  $\Delta t$ . The laser field intensity at the focal spot was estimated to be  $2.1(2) \times 10^{14}$  W/cm<sup>2</sup> from the pulse energy, pulse duration and focal spot size.

## 3. Results and discussion

### 3.1. Extraction of pump-probe signals

Figure 1(a) and (b) shows the distributions of the released kinetic energy  $E_{\text{kin}}$  as a function of  $\Delta t$  in the Coulomb explosion pathways (1) and (2), respectively. These  $E_{\text{kin}}$  distributions also include contributions from the signals generated by the pump laser pulses only and those by the probe laser pulses only. This is because methanol dications ( $\text{CH}_3\text{OH}^{2+}$ ) can also be generated by a single pulse and the fragment ions can be produced by the Coulomb explosion processes of  $\text{CH}_3\text{OH}^{2+}$ . In order to subtract the effect of this single pulse double ionization, the  $E_{\text{kin}}$  distributions were measured using the pump laser pulses or the probe laser pulses only. The results are shown in Figure 2(a) and (b) for the non-migration pathways (1) and (2), respectively.

In the pump-probe measurements, after a pump laser pulse ionizes molecules in a sample gas, the number of neutral molecules decreases to a certain extent. If the number of neutral molecules  $N$  within the interaction volume decreases to  $\alpha N$  ( $\alpha < 1$ ), the yield of doubly ionized molecules produced by a probe laser pulse should also decrease by a factor of  $\alpha$  in comparison to the yield of the doubly ionized molecules generated by a pump laser pulse. In order to account for this depletion effect induced by the pump laser pulses in the pump-probe measurements, the red curves in Figure 2(a) and (b) were obtained as a weighted sum of the ion yields defined as

$$I_{\text{weighted}} = I_{\text{pump}} + \alpha I_{\text{probe}} \quad (5)$$

where  $I_{\text{pump}}$  represents the total yield of ions generated by the pump laser pulses only and  $I_{\text{probe}}$  represents the total yield of the ions generated by the probe laser pulses only. Under the present experimental conditions, the factor  $\alpha$  was estimated to be 0.79(5) as the averaged value of  $\alpha$  obtained by the two separate sets of the measurements of the total ion yields obtained by (i) pump laser pulses only, (ii) probe laser pulses only, and (iii) pump and probe pulses with  $\Delta t=430$  fs.

Figure 2(c) and (d) shows respectively the  $E_{\text{kin}}$  distributions of the non-migration pathway and the migration pathway obtained by subtracting the weighted sum of the  $E_{\text{kin}}$  distribution from the  $E_{\text{kin}}$  distribution obtained by the pump-probe experiment when  $\Delta t=430$  fs. Therefore, the  $E_{\text{kin}}$  distributions in Figure 2(c) and (d) can be regarded as those originating from the sequential ionization

Download English Version:

<https://daneshyari.com/en/article/5380203>

Download Persian Version:

<https://daneshyari.com/article/5380203>

[Daneshyari.com](https://daneshyari.com)